Available online at www.sciencedirect.com
SCIENCE DIRECT®
Bioorganic & Medicinal Chemistry Letters 14 (2004) 4897–4902
Bioorganic & Medicinal Chemistry Letters

Potent and selective P^2–P^3 ketoamide inhibitors of cathepsin K with good pharmacokinetic properties via favorable $P^{1'}$, P^1, and/or P^3 substitutions

David G. Barrett,[a,†] John G. Catalano,[a,*] David N. Deaton,[a] Anne M. Hassell,[b] Stacey T. Long,[c] Aaron B. Miller,[b] Larry R. Miller,[d] Lisa M. Shewchuk,[b] Kevin J. Wells-Knecht,[e] Derril H. Willard, Jr.[f,✠] and Lois L. Wright[g]

[a]*Department of Medicinal Chemistry, GlaxoSmithKline, Research Triangle Park, NC 27709, USA*
[b]*Discovery Research Computational, Analytic, and Structural Sciences, GlaxoSmithKline, Research Triangle Park, NC 27709, USA*
[c]*Department of World Wide Physical Properties, GlaxoSmithKline, Research Triangle Park, NC 27709, USA*
[d]*Department of Molecular Pharmacology, GlaxoSmithKline, Research Triangle Park, NC 27709, USA*
[e]*Department of Research Bioanalysis and Drug Metabolism, GlaxoSmithKline, Research Triangle Park, NC 27709, USA*
[f]*Department of Gene Expression and Protein Purification, GlaxoSmithKline, Research Triangle Park, NC 27709, USA*
[g]*Discovery Research Biology, GlaxoSmithKline, Research Triangle Park, NC 27709, USA*

Received 18 May 2004; revised 13 July 2004; accepted 17 July 2004
Available online 4 August 2004

Abstract—A series of ketoamides were synthesized and evaluated for inhibitory activity against cathepsin K. Exploration of the interactions between achiral P^2 substituents and the cysteine protease based on molecular modelling suggestions resulted in potent cathepsin K inhibitors that demonstrated high selectivity versus cathepsins B, H, and L. Subsequent modifications of the P^3, P^1, and $P^{1'}$ moieties afforded orally bioavailable inhibitors.

Healthy bone tissue is maintained by specialized cells called osteoclasts and osteoblasts.[1] These cells operate in concert by continuously remodelling bone tissue in a process of bone resorption by osteoclasts and bone formation by osteoblasts. Osteoclasts affect resorption by secreting acid and proteolytic enzymes to degrade the mineral and matrix components of bone, respectively. Healthy bone maintains equilibrium between the bone resorption and bone formation processes. Bone becomes susceptible to osteoporosis and fracture when bone degradation significantly outpaces bone formation. A potentially promising strategy to correct such an imbalance is to slow bone degradation by inhibiting cathepsin K, the main proteolytic enzyme secreted by osteoclasts to break down type I collagen, the primary component of bone matrix.[2] Small molecule inhibitors of cathepsin K, a cysteine protease, have shown promise in attenuating bone resorption in osteoporosis animal models.[3]

This group has previously reported potent small molecule cathepsin K inhibitors based on aldehyde and α-ketoamide electrophiles.[4–8] Inhibitors such as α-ketoamide **1** (IC_{50} = 1.1 nM) bind directly to the active site of cathepsin K. Binding modes for these molecules were clearly defined through molecular modelling constructs designed directly from inhibitor-bound enzyme crystal structures.[4,5,8] The reactive cysteine thiol of the enzyme forms a reversible covalent bond with the α-ketoamide moiety and the bulky *t*-butyl group at P^2 effectively fills the hydrophobic S^2 enzyme subsite. The S^2 subsite of cathepsin K is the deepest, most pronounced hydrophobic binding pocket of the cathepsin K active site and contains key structural variances over other human cysteine cathepsin family members.[9] The P^3 phenyl group

Keywords: Cathepsin K; Ketoamide; Cysteine protease inhibitor.
* Corresponding author. Tel.: +1-919-483-6264; fax: +1-919-483-6053; e-mail: john.g.catalano@gsk.com
† Present address: Lilly Forschung GmbH, Essener Street 93, 22419 Hamburg, Germany.
✠ Deceased.

0960-894X/$ - see front matter © 2004 Elsevier Ltd. All rights reserved.
doi:10.1016/j.bmcl.2004.07.031

of **1** adds an additional interaction for binding. These significant binding sites warranted further SAR exploration of the P^2–P^3 substituents. Modelling studies suggested that achiral P^2–P^3 groups such as in **2** had potential to bind favorably at the S^2–S^3 subsites of cathepsin K.[10] To circumvent the need for asymmetric syntheses or efficient chiral separations required for the preparation of inhibitors such as **1**, analogs with achiral groups were studied.

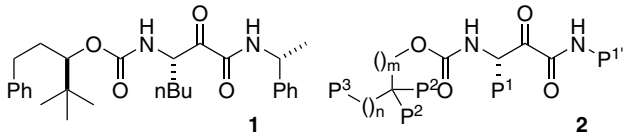

1 **2**

Additionally, it was desired to incorporate hydrophilic groups into the inhibitors to promote greater water solubility and a more favorable pharmacokinetic profile. Although hydrophilic substituents are not well tolerated at S^2, molecular modelling and previous SAR studies suggested that heteroatom substitution would likely be tolerated at P^3, P^1, and $P^{1'}$.[4,8,10] The *n*-butyl P^1 substituent in **1** runs the length of a shallow hydrophobic groove that extends roughly four carbon–carbon bond lengths and then gives way to solvent, thereby allowing an opportunity to introduce hydrophilic groups. The S^3 site is hydrophobic in nature, but more solvent exposed than S^2. The P^3 position was therefore also considered for incorporating water-solubilizing groups. Previous SAR studies showed that $S^{1'}$ would also accept hydrophilic substitution.

As shown in Scheme 1, the first process to synthesize ketoamides applied the acyl cyanophosphorane oxidative cleavage and amine coupling procedure of Wasserman and Petersen.[11] Coupling of the known isocyanate **3**[6] with commercially available alcohols **4a** and **4d**–**e** or known alcohols **4b**–**c**[12] afforded carbamate esters that were hydrolyzed to the acids **5a**–**e**. Coupling the acids **5a**–**e** with cyanomethyltriphenylphosphonium ylide yielded phosphoranes **6a**–**e**. Oxidative cleavage of the carbon–phosphorous bond generated reactive acyl cyanophosphoranes that were coupled with (*R*)-1-phenylethylamine or 3-aminopyrazole to give the desired α-ketoamides **2a**–**e**, and **2l**.

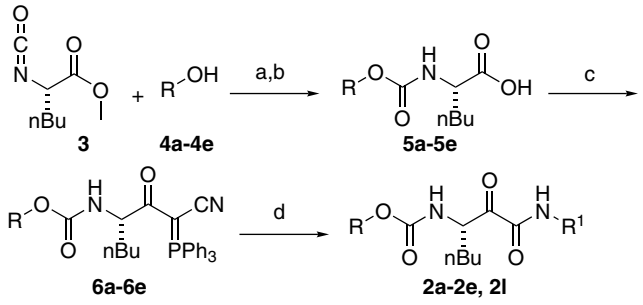

Scheme 1. Reagents and conditions: (a) ROH, PhMe, 85 °C, sealed tube, 89–99%; (b) LiOH·H_2O, THF, H_2O; 1 N HCl; (c) $Ph_3P{=}CCN$, DMAP, EDC, CH_2Cl_2, 46–79% over two reactions; (d) O_3, CH_2Cl_2, −78 °C; N_2; R^1NH_2, −78 °C to rt; $AgNO_3$, THF, H_2O, 19–45%.

The P^2–P^3 alcohols used for the synthesis of **2h**–**k** (Table 1) and **2l**–**p** (Table 2) were prepared as in Scheme 2. The enolates of ethyl cyclobutane carboxylate or methyl cyclopentane carboxylate **7** were formed by treatment with LDA. The enolates thus formed were coupled with preferred P^3 bromomethyl arenes to give esters **8**. Lithium aluminum hydride reductions of **8** provided desired P^2–P^3 alcohols **9**.

Ketoamides **2f**–**k** were synthesized as in Scheme 3. Treatment of P^2–P^3 alcohols with phosgene yielded chloroformates that were coupled with the previous described amino alcohols **10**.[6] Subsequent oxidation provided the α-ketoamides **2f**–**k**.

Table 1. Inhibition of human cathepsin K by P^2–P^3 analogs

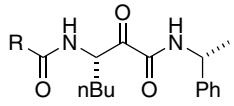

#	R	IC_{50} (nM)[a]
2a	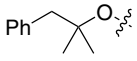	630
2b	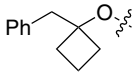	710
2c	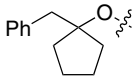	25
2d	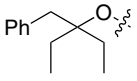	150
2e	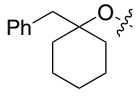	210
2f	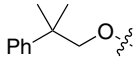	65
2g	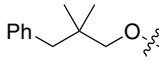	13
2h	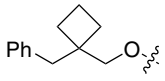	8.5
2i	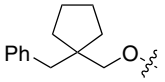	26
2j	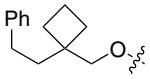	24
2k	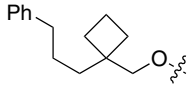	17

[a] Inhibition of recombinant human cathepsin K activity in a fluorescence assay using 10 μM Cbz-Phe-Arg-AMC as substrate in 100 mM NaOAc, 10 mM DTT, 120 mM NaCl, pH = 5.5. The IC_{50} values are the mean of two or three inhibition assays, individual data points in each experiment were within a 3-fold range of each other.

Table 2. Inhibition of human cathepsin K by combination analogs

#	R	IC_{50} (nM)[a]
2l	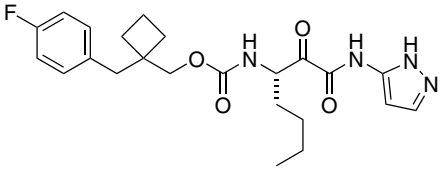	0.83
2m	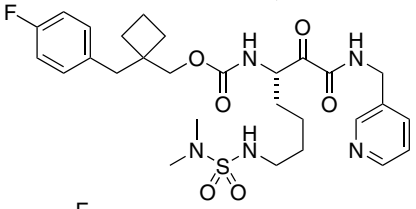	40
2n	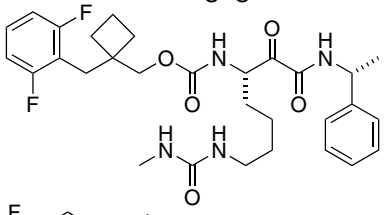	24
2o	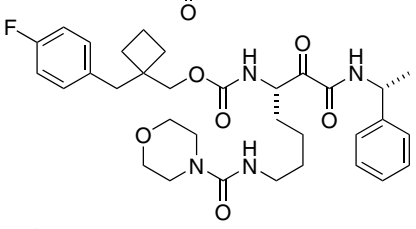	13
2p	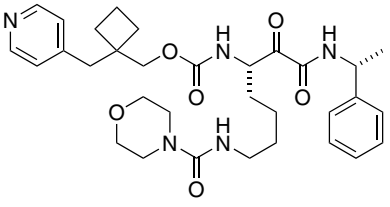	7.6

[a] Inhibition of recombinant human cathepsin K activity in a fluorescence assay using 10 μM Cbz-Phe-Arg-AMC as substrate in 100 mM NaOAc, 10 mM DTT, 120 mM NaCl, pH = 5.5. The IC_{50} values are the mean of two or three inhibition assays, individual data points in each experiment were within a 3-fold range of each other.

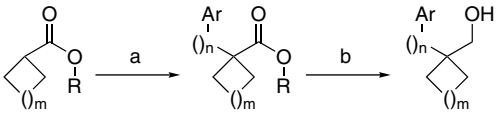

7 **8** **9**

Scheme 2. Reagents and conditions: (a) Di-*iso*-propylamine, 1.6 M *n*-BuLi, −78 to 0 °C, THF; $ArCH_2Br$, 75–90%; (b) $LiAlH_4$, THF, 0 °C, 25–90%.

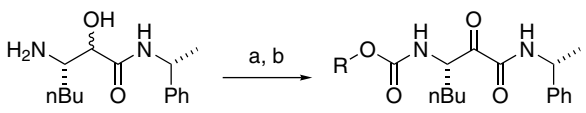

10 **2f-2k**

Scheme 3. Reagents and conditions: (a) ROH, 1.93 M $COCl_2$ in PhMe, pyridine, CH_2Cl_2, −20 °C to rt; **10**, *i*-Pr_2NEt, dioxane, 22–91%; (b) Dess–Martin periodinane, CH_2Cl_2, 55–78%.

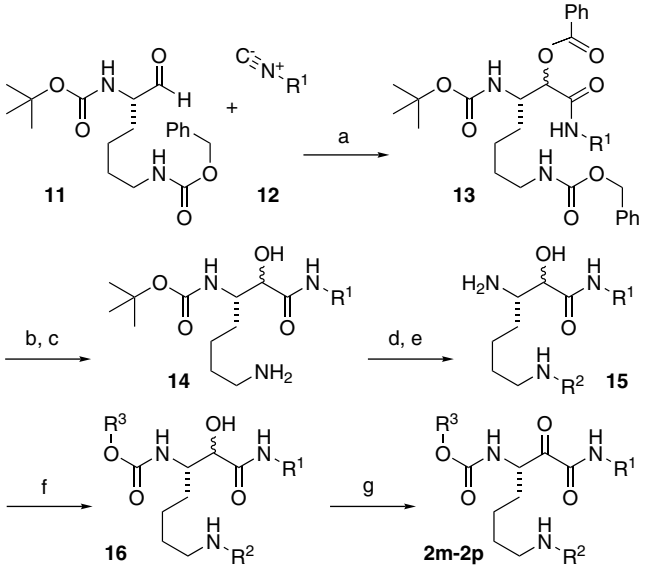

11 **12** **13** **14** **15** **16** **2m-2p**

Scheme 4. Reagents and conditions: (a) R^1NC, PhCOOH, CH_2Cl_2, 60–65%; (b) $LiOH{\cdot}H_2O$, dioxane, H_2O, 100 °C, 86–95%; (c) 10% Pd/C, EtOH, 40 psi H_2, 99% (d) MeN=C=O or Me_2NSO_2Cl or 4-morpholinecarbonyl chloride, NEt_3, THF, 48–80%; (e) HCl(g), EtOAc, 0 °C, 99%; (f) R^3OH, 1.93 M $COCl_2$ in PhMe, THF, −20 °C to rt; **17**, Et_3N, THF, 30–59%; (g) $(COCl)_2$, CH_2Cl_2, DMSO, Et_3N, −60 °C to rt, 42–77%.

Another route exploited the Passerini reaction to synthesize inhibitors **2m–p** as shown in Scheme 4.[13] $P^{1'}$ isocyanides **12** were synthesized from amines under known conditions[14] and reacted with aldehyde **11** using Passerini conditions to yield **13**. Acyloxyamides **13** were hydrolyzed with aqueous lithium hydroxide, and the benzyl carbamate protecting group was removed under hydrogenolysis conditions to give amines **14**. Amines **14** were coupled with dimethylsulfamoyl chloride, methyl isocyanate, or 4-morpholinecarbonyl chloride to introduce the P^1 substituent before Boc removal with hydrogen chloride in ethyl acetate yielded amino alcohols **15**. P^2–P^3 chloroformates were coupled with **15** to provide alcohols **16**. Subsequent Swern oxidation provided α-ketoamides **2m–p**.

As shown in Table 1, compounds **2a–e** incorporated achiral P^2 tertiary carbamates to occupy the S^2 pocket, and included a fixed benzyl group extending out towards S^3. Dimethyl and cyclobutyl P^2 analogs, **2a** (IC_{50} = 630 nM) and **2b** (IC_{50} = 710 nM) respectively, were only moderately active against cathepsin K. The relative geometry and smaller size of these P^2 groups seemingly prevent an optimal binding interaction at S^2. The increased P^2 bulk of cyclopentyl analog **2c** (IC_{50} = 25 nM), however, translated into a significant potency boost over **2a** and **2b**. The P^2 diethyl group of **2d** (IC_{50} = 150 nM) presumably may only use a single ethyl group to interact with S^2 as it is significantly less potent than **2c**. Potency was also reduced by increasing the size of the P^2 substituent as in cyclohexyl analog **2e** (IC_{50} = 210 nM).

Further molecular modelling suggested that the P^2 moieties of **2a–e** did not extend far enough to fully access

the S^2 pocket. Inhibitor **2f** (IC_{50} = 65 nM) was synthesized for direct comparison to **2a** and included a one atom shift of P^2 substituent. The ~10-fold increase in potency observed for **2f** over **2a** reinforced the molecular modelling studies. Modelling also suggested that extending the P^3 linker would enhance S^3 subsite interactions. Increasing the linker between P^2 and P^3 by one atom as in **2g** (IC_{50} = 13 nM) resulted in an additional 5-fold increase in potency. The cyclobutyl analog **2h** (IC_{50} = 8.5 nM) was equally active, but additional increases in the size of P^2 as in **2i** (IC_{50} = 26 nM) did not increase potency. Extending the phenyl group further towards S^3, as with **2j** (IC_{50} = 24 nM) and **2k** (IC_{50} = 17 nM), gave equivalent activity versus cathepsin K. These last two inhibitors must pay a higher entropic cost upon binding to the cathepsin K active site. Although conformational constraints to the P^2–P^3 linker could reduce this cost and might enhance activity, those changes would increase size and reduce solubility and were not pursued.

Having achieved reasonable inhibitory activity against cathepsin K, focus shifted towards improving the pharmacokinetic profile of these molecules. With highly lipophilic molecules such as **2a**–**k**, aqueous solubility and oral bioavailability were obvious concerns. Utilizing SAR from previous ketoamide inhibitors,[6,8] hydrophilic moieties were substituted, singly or in combination, at $P^{1'}$, P^1, and P^3 to enhance solubility. Furthermore, potential metabolic sites were also altered. The resulting analogs **2l**–**p** are shown in Table 2. The $P^{1'}$ pyrazole-containing analog **2l** (IC_{50} = 0.83 nM) exhibited enhanced potency versus **2h**,[8] whereas the $P^{1'}$ pyridine-containing analog **2m** (IC_{50} = 40 nM) showed decreased activity relative to **2h**.[7] P^1 lysine derivatives **2n**–**o** and the P^3 pyridine **2p** did not significantly alter inhibitory activity.

As shown in Table 3, all inhibitors in this series displayed excellent selectivity for cathepsin K versus cathepsin B and cathepsin H. Although reasonable selectivity was also achieved against cathepsin L, several inhibitors such as **2f** (L/K = 46) and **2o** (L/K = 28) were less selective versus this enzyme. Furthermore, these inhibitors showed little selectivity versus cathepsin S, with the cyclopentyl analog **2i** being an apparently more potent cathepsin S inhibitor. These results were not too surprising since cathepsin K is structurally more similar to the endopeptidases cathepsin L and cathepsin S than the exopeptidases cathepsin B and cathepsin H.[15]

Cell permeability, solubility, and pharmacokinetic parameters for analogs **2l**–**p** are depicted in Table 4. With the exception of **2p** (P_{APP} = 14 nm/sec), all of these analogs exhibited good permeability in Madin–Darby canine kidney cell monolayer assays (P_{APP} = 69–470 nm/sec).[16] Inhibitors **2m** (FS-SIF Sol. = 0.032 mg/mL, F = 18%) and **2n** (FS-SIF Sol. = 0.027 mg/mL, F = 15%) were poorly soluble in fasted state-simulated intestinal fluid,[17] and this probably contributes to their moderate oral bioavailability in male Han–Wistar rats. Analogs **2l** (FS-SIF Sol. = 0.15 mg/mL, F = 31%) and **2o** (FS-SIF Sol. = 0.098 mg/mL, F = 38%) exhibited 3- to 5-fold increases in solubility compared to **2m** and **2n** and resulted in a doubling of oral bioavailability. Although **2p** (FS-SIF Sol. = 0.30 mg/mL) was the most soluble analog, its moderate membrane permeability (P_{APP} = 14 nm/sec) presumably limits oral bioavailability (F = 8.1%). The total clearance of analog **2m** was low (C_l = 9.6 mL/min/kg), leading to a long terminal half-life ($t_{1/2}$ = 270 min) despite a moderate volume of distribution (V_{SS} = 420 mL/kg). The other inhibitors were more rapidly eliminated (C_l = 27–45 mL/min/kg) resulting in shorter half-lifes ($t_{1/2}$ = 74–120 min) even though the volumes were enhanced (V_{SS} = 660–4200 mL/kg). Of particular notice, analog **2l** was an extremely potent cathepsin K inhibitor that demonstrated good oral bioavailability in rats.

Subsequent to the above work, an X-ray co-crystal structure of cathepsin K with inhibitor **2l** was solved and the active site is shown in Figure 1. A covalent hemithioketal intermediate is formed by the α-keto moiety of

Table 3. Selectivity of cathepsin K inhibitor analogs

#	Cat B IC_{50} (nM)[a]	Cat H IC_{50} (nM)[b]	Cat L IC_{50} (nM)[c]	Cat S IC_{50} (nM)[d]	B/K	H/K	L/K	S/K
2c	>12,000	>12,000	3000	430	>480	>480	120	17
2f	>5000	>5000	3000	270	>77	>77	46	4.2
2g	>5000	>5000	1200	20	>380	>380	92	1.5
2h	3600	>5000	1300	20	420	>580	150	2.4
2i	>5000	>5000	2200	11	>190	>190	85	0.4
2j	>2000	>2000	1600	34	>83	>83	67	1.4
2k	>2000	>2000	1300	17	>120	>120	76	1.0
2l	>500	>500	330	5.2	>600	>600	390	6.3
2m	>5000	>5000	>5000	130	>120	>120	>120	3.2
2o	>5000	>5000	680	27	>200	>200	28	2.1

[a] Inhibition of recombinant human cathepsin B activity in a fluorescence assay using 10 μM Cbz-Phe-Arg-AMC as substrate in 100 mM NaOAc, 10 mM DTT, 120 mM NaCl, pH = 5.5.

[b] Inhibition of recombinant human cathepsin H activity in a fluorescence assay using 50 μM L-Arg-β-naphthalamide as substrate in 100 mM NaOAc, 10 mM DTT, 120 mM NaCl, pH = 5.5.

[c] Inhibition of recombinant human cathepsin L activity in a fluorescence assay using 5 μM Cbz-Phe-Arg-AMC as substrate in 100 mM NaOAc, 10 mM DTT, 120 mM NaCl, pH = 5.5.

[d] Inhibition of recombinant human cathepsin S activity in a fluorescence assay using 10 μM Cbz-Val-Val-Arg-AMC as substrate in 100 mM NaOAc, 10 mM DTT, 120 mM NaCl, pH = 5.5.

Table 4. Pharmacokinetics of combination analogs

#	MDCK[a] P_{APP}[b] (nm/sec)	Sol. FS-SIF[c] (mg/mL)	$t_{1/2}$[d] (min)	C_l[h] (mL/min/kg)	V_{SS}[i] (mL/kg)	F[j] (%)
2l	150	0.15	120[e]	45	—	31
2m	69	0.032	270[f]	9.6	420	18
2n	140	0.027	94[e]	33	1600	15
2o	470	0.098	110[g]	43	4200	38
2p	14	0.30	74[g]	27	660	8.1

[a] Madin–Darby canine kidney cell monolayer transport assay.
[b] P_{APP} is the apparent permeability coefficient for apical to basoplateral flux in nanometers per second.
[c] FS-SIF is the equilibrium solubility in fasted state-simulated intestinal fluid.
[d] $t_{1/2}$ is the iv terminal half-life dosed as a solution.
[e] Dosed as a solution in 30% hydroxypropyl-β-cyclodextrin, pH = 5.1.
[f] Dosed as a solution in 30% sulfobutylether-β-cyclodextrin, pH = 3.5.
[g] Dosed as a solution in 40% hydroxypropyl-β-cyclodextrin, pH = 5.1.
[h] C_l is the total clearance.
[i] V_{SS} is the steady state volume of distribution.
[j] F is the oral bioavailability.

the inhibitor and the active site ^{25}Cys of the enzyme. This is consistent with the reversible nature of these time-dependent, tight binding inhibitors. As in other ketoamide co-crystal structures from this group, the hemithioketal hydroxyl is stabilized by hydrogen bonds to the catalytic histidine (^{162}His) and the backbone carbonyl of ^{161}Asn, but does not occupy the oxy-anion hole.[8] Thus, the active site thiol attacks the carbonyl with opposite stereochemistry from published aldehyde and ketone cathepsin K structures.[5,18] Instead, the carbonyl of the amide rests in the oxyanion hole where it is stabilized by hydrogen bonds to the side chain NH of ^{19}Gln and the backbone NH of ^{25}Cys. The carbamate also forms two hydrogen bonds with the peptide backbone recognition site of the enzyme. Thus, the carbamate NH donates a hydrogen bond to ^{161}Asn, while the carbamate carbonyl accepts a hydrogen bond from the backbone NH of ^{66}Gly. Furthermore, the P$^{1'}$ pyrazole forms a final hydrogen bond to the ^{184}Trp indole NH.

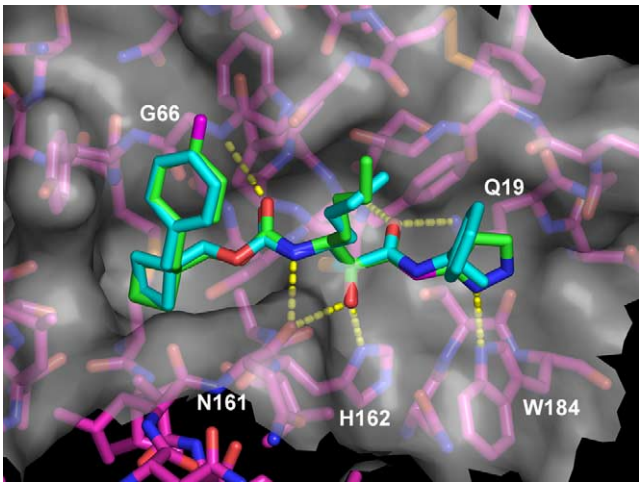

Figure. 1. Active site of the X-ray co-crystal structure of compound **2l** complexed with cathepsin K. The cathepsin K carbons are colored magenta with inhibitor **2l** carbons colored green. The semi-transparent white surface represents the molecular surface, while hydrogen bonds are depicted as yellow dashed lines. The original modeled structure of inhibitor **2h**, with its carbons colored cyan, is also shown in the figure. The coordinates have been deposited in the Brookhaven Protein Data Bank, accession number 1TU6. This figure was generated using PYMOL version 0.93 (Delano Scientific, www.pymol.org).

Besides these hydrogen bond stabilizing interactions with the protein, the norleucine-derived P^1 group of the inhibitor faces the S^1 wall formed from ^{23}Gly, ^{24}Ser, ^{64}Gly, and ^{65}Gly, with one side of the *n*-butyl group forming van der Waals interactions with the protease while its terminal carbon is exposed to solvent. Moreover, the P^2 cyclobutyl group forms hydrophobic interactions with the S^2 pocket composed of ^{67}Tyr, ^{68}Met, ^{134}Ala, ^{163}Ala, and ^{209}Leu. The cyclobutyl P^2 moiety occupation of the only deep pocket in the protease is not as favorable as in the case of the asymmetrically directed P^2 substituents exemplified by **1**. This discrepancy, arising from the P^2 cyclobutyl projecting one atom further down the inhibitor backbone than the asymmetric P^2 *t*-butyl and at a different angle, may account for the slight decrease in potency between **1** (IC_{50} = 1.1 nM) and **2h** (IC_{50} = 8.5 nM). Finally, the P^3 phenyl extends toward the S^3 groove framed by ^{60}Asn, ^{61}Asp, ^{66}Gly, and ^{67}Tyr, making hydrophobic contacts with this trough.

The original modeled structure of analog **2h** docked into the cathepsin K structure with the MVP modelling program is also depicted.[10] The inhibitor was docked into the active site by growing the ligand in a covalently attached state, starting at the β-carbon of ^{25}Cys. There is excellent agreement between the modeled structure of **2h** and the solved structure of **2l**. This modelling was undertaken to assist in designing achiral P^2–P^3 moieties. The bound and modeled P^3 phenyl groups occupy virtually identical space, while the distal part of the modeled P^2 cyclobutyl substituent is only slightly skewed from the bound cyclobutyl. The difference may reflect movement of the protein to best accommodate the inhibitor, since the modelling uses a constrained enzyme. The exceptional harmony between the modeled and bound structures and the usefulness of docking potential inhibitors to identify novel and potent P^2–P^3 moieties further attests to the utility of this approach in lead development.

In summary, this article describes SAR studies for a potent series of cathepsin K inhibitors. Incorporation of achiral P^2–P^3 substituents, based on molecular modelling suggestions, afforded good inhibitory activity versus cathepsin K. Furthermore, modifications to $P^{1'}$, P^1, and P^3 groups, designed to enhance solubility and permeability, and to block potential sites of metabolism, improved pharmacokinetic properties. The resulting inhibitors exhibited good to excellent selectivity versus cathepsins B, H, and L. These studies resulted in the discovery of potent and selective inhibitors like **2l** that demonstrated good oral bioavailability.

References and notes

1. Einhorn, T. A. In *Osteoporosis*; Marcus, R., Feldman, D., Kelsey, J., Eds.; Academic: San Diego, California, 1996; p 3.
2. Deaton, D. N.; Kumar, S. **2004**, *42*, 245, p 245.
3. Stroup, G. B.; Lark, M. W.; Veber, D. F.; Bhattacharyya, A.; Blake, S.; Dare, L. C.; Erhard, K. F.; Hoffman, S. J.; James, I. E.; Marquis, R. W.; Ru, Y.; Vasko-Moser, J. A.; Smith, B. R.; Tomaszek, T.; Gowen, M. *J. Bone Miner. Res.* **2001**, *16*, 1739.
4. Catalano, J. G.; Deaton, D. N.; Furfine, E. S.; Hassell, A. M.; McFadyen, R. B.; Miller, A. B.; Miller, L. R.; Shewchuk, L. M.; Willard, D. H.; Wright, L. L. *Bioorg. Med. Chem. Lett.* **2004**, *14*, 275.
5. Boros, E. E.; Deaton, D. N.; Hassell, A. M.; McFadyen, R. B.; Miller, A. B.; Miller, L. R.; Paulick, M. G.; Shewchuk, L. M.; Thompson, J. B.; Willard, D. H.; Wright, L. L. *Bioorg. Med. Chem. Lett.* **2004**, *14*, 3425.
6. Catalano, J. G.; Deaton, D. N.; Long, S. T.; McFadyen, R. B.; Miller, L. R.; Payne, J. A.; Wells-Knecht, K. J.; Wright, L. L. *Bioorg. Med. Chem. Lett.* **2004**, *14*, 719.
7. Barrett, D. G.; Catalano, J. G.; Deaton, D. N.; Long, S. T.; Miller, L. R.; Tavares, F. X.; Wells-Knecht, K. J.; Wright, L. L.; Zhou, H.-Q. Q. *Bioorg. Med. Chem. Lett.* **2004**, *14*, 2543.
8. Tavares, F. X.; Boncek, V.; Deaton, D. N.; Hassell, A. M.; Long, S. T.; Miller, A. B.; Payne, A. A.; Miller, L. R.; Shewchuk, L. M.; Wells-Knecht, K.; Willard, D. H., Jr.; Wright, L. L.; Zhou, H.-Q. *J. Med. Chem.* **2004**, *47*, 588.
9. Turk, D.; Guncar, G.; Podobnik, M.; Turk, B. *Biol. Chem.* **1998**, *379*, 137.
10. Lambert, M. H. In *Practical Application of Computer-Aided Drug Design*; Charifson, P. S., Ed.; Marcel Dekker: New York, 1997; p 243.
11. Wasserman, H. H.; Petersen, A. K. *J. Org. Chem.* **1997**, *62*, 8972.
12. Finkel'shtein, E. S.; Mikaya, A. I.; Zaikin, V. G.; Vdovin, V. M. *Neftekhimiya* **1980**, *20*, 75.
13. Semple, J. E.; Owens, T. D.; Nguyen, K.; Levy, O. E. *Org. Lett.* **2000**, *2*, 2769.
14. Weber, W. P.; Gokel, G. W. *Tetrahedron Lett.*, **1972**, 1637.
15. Somoza, J. R.; Palmer, J. T.; Ho, J. D. *J. Mol. Biol.* **2002**, *322*, 559.
16. Irvine, J. D.; Takahashi, L.; Lockhart, K.; Cheong, J.; Tolan, J. W.; Selick, H. E.; Grove, J. R. *J. Pharm. Sci.* **1999**, *88*, 28.
17. Dressman, J. B.; Amidon, G. L.; Reppas, C.; Shah, V. P. *Pharm. Res.* **1998**, *15*, 11.
18. Marquis, R. W.; Ru, Y.; LoCastro, S. M.; Zeng, J.; Yamashita, D. S.; Oh, H.-J.; Erhard, K. F.; Davis, L. D.; Tomaszek, T. A.; Tew, D.; Salyers, K.; Proksch, J.; Ward, K.; Smith, B.; Levy, M.; Cummings, M. D.; Haltiwanger, R. C.; Trescher, G.; Wang, B.; Hemling, M. E.; Quinn, C. J.; Cheng, H. Y.; Lin, F.; Smith, W. W.; Janson, C. A.; Zhao, B.; McQueney, M. S.; D'Alessio, K.; Lee, C.-P.; Marzulli, A.; Dodds, R. A.; Blake, S.; Hwang, S.-M.; James, I. E.; Gress, C. J.; Bradley, B. R.; Lark, M. W.; Gowen, M.; Veber, D. F. *J. Med. Chem.* **2001**, *44*, 1380.